



RESEARCH LETTER

10.1002/2017GL074270

Key Points:

- Additional limits placed on potential length and location of future large earthquakes along the Himalayan Frontal Thrust
- Dip-slip displacement of ~11 m on Himalayan Frontal Thrust (HFT) in eastern Nepal occurred roughly 800 years ago in 1146–1256 A.D.
- Slip now accumulated along Main Himalayan Thrust (MHT) of eastern Nepal to produce another earthquake similar to event of ~800 years ago

Supporting Information:

- Supporting Information S1

Correspondence to:

S. G. Wesnousky,
wesnousky@unr.edu

Citation:

Wesnousky, S. G., Y. Kumahara, D. Chamlagain, I. K. Pierce, T. Reedy, S. J. Angster, and B. Giri (2017), Large paleoearthquake timing and displacement near Damak in eastern Nepal on the Himalayan Frontal Thrust, *Geophys. Res. Lett.*, 44, 8219–8226, doi:10.1002/2017GL074270.

Received 22 MAY 2017

Accepted 26 JUL 2017

Accepted article online 31 JUL 2017

Published online 19 AUG 2017

Large paleoearthquake timing and displacement near Damak in eastern Nepal on the Himalayan Frontal Thrust

Steven G. Wesnousky¹ , Yasuhiro Kumahara² , Deepak Chamlagain^{1,3} , Ian K. Pierce¹ , Tabor Reedy¹ , Stephen J. Angster¹ , and Bibek Giri⁴

¹Center for Neotectonic Studies and Seismological Laboratory, University of Nevada, Reno, Nevada, USA, ²Graduate School of Education, Hiroshima University, Hiroshima, Japan, ³Department of Geology, Tri-Chandra Multiple Campus, Kathmandu, Nepal, ⁴Central Department of Geology, Tribhuvan University, Kirtipur, Nepal

Abstract An excavation across the Himalayan Frontal Thrust near Damak in eastern Nepal shows displacement on a fault plane dipping ~22° has produced vertical separation across a scarp equal to 5.5 m. Stratigraphic, structural, geometrical, and radiocarbon observations are interpreted to indicate that the displacement is the result of a single earthquake of 11.3 ± 3.5 m of dip-slip displacement that occurred 1146–1256 A.D. Empirical scaling laws indicate that thrust earthquakes characterized by average displacements of this size may produce rupture lengths of 450 to >800 km and moment magnitudes M_w of 8.6 to >9. Sufficient strain has accumulated along this portion of the Himalayan arc during the roughly 800 years since the 1146–1256 A.D. earthquake to produce another earthquake displacement of similar size.

Plain Language Summary The densely populated country of Nepal sits above the Himalayan Frontal Thrust fault. It is repeated displacements on this fault that are responsible for the uplift of the Himalaya mountains and considered capable of producing great earthquakes. Here we excavate a trench across the fault to show a great earthquake occurred 1146–1256 AD in eastern Nepal. It has been a sufficiently long time since then that stresses have accumulated to a level capable of producing another such great earthquake.

1. Introduction

The trace of the Himalayan Frontal Thrust (HFT) strikes southeastward for a distance of ~800 km along the southern border of Nepal (Figure 1). The fault dips northward to form the Main Himalayan Thrust (MHT), a shallow decollement that extends ~120 km toward the High Himalaya [Seeber and Armbruster, 1981]. The northward limit of the locked portion of the decollement is marked by a zone of moderate seismicity that trends southeastward across Nepal (Figure 1) [e.g., Avouac *et al.*, 2015]. The locked portion of the MHT is considered to slip only during repeated large earthquakes that accommodate ~20 mm/yr of convergence between India and Tibet [e.g., Bilham *et al.*, 1997]. Large historical earthquakes interpreted or speculated to have produced displacement on the MHT of Nepal include the M_w ~8.4 1934 Bihar earthquake [Molnar and Deng, 1984], the M_w 7.8 2015 Gorkha earthquake [Hayes *et al.*, 2015], the M_s > 8 earthquake of July 6, 1505 [Ambraseys and Jackson, 2003], and several events that produced damage in Kathmandu in 1255 A.D., 1344 A.D., and 1408 A.D. [Bollinger *et al.*, 2016; Pant, 2002]. Surface rupture correlated to the 1934 earthquake at Sir Khola has been inferred to have continued at least 150 km farther eastward along the HFT (red line in Figure 1) [Sapkota *et al.*, 2013]. The 2015 M_w 7.8 Gorkha earthquake rupture was confined to a downdip section of the locked portion of the MHT [Avouac *et al.*, 2015; Hayes *et al.*, 2015]. Potentially greater earthquakes may rupture farther updip to encompass the entire width of the locked zone along the HFT. A number of studies are now reported along the HFT assessing the age, size, and recurrence time of prehistoric earthquakes that have produced surface rupture (2006) [Kumar *et al.*, 2006, 2010; Lave *et al.*, 2005; Le Roux-Mallouf *et al.*, 2016; Mugnier *et al.*, 2005; Nakata *et al.*, 1998; Wesnousky *et al.*, 1999, 2017; Yule *et al.*, 2006]. We add to these reports a description of our recent findings arising from study of a trench excavated across the HFT near Damak. After describing the location of the site and our observations, we conclude with a discussion of our interpretations in the context of prior similar studies along the HFT of Nepal.

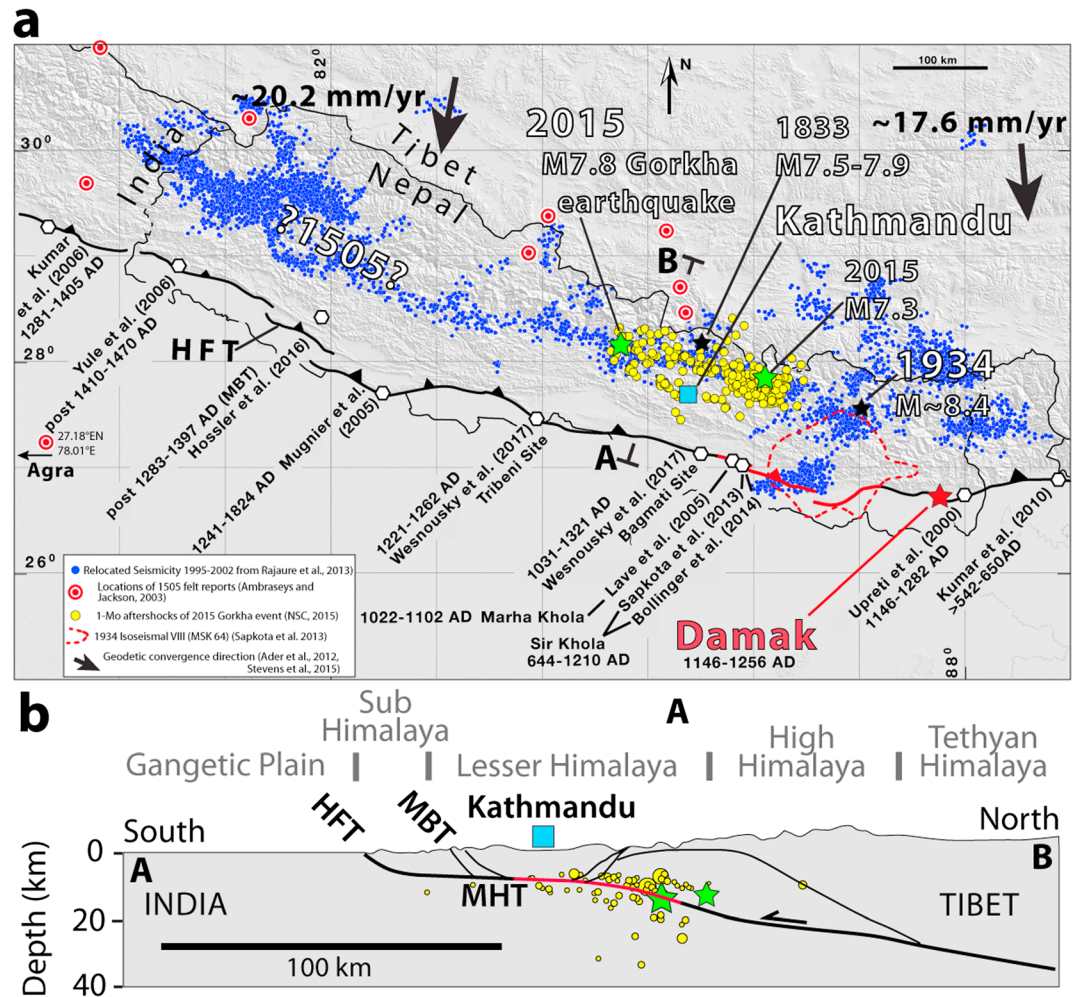


Figure 1. (a) Location of Damak and age of surface rupture earthquakes reported at sites along the Himalayan Frontal Thrust (HFT). (b) Generalized cross section along trend AB (shown in Figure 1a) adapted from *Lave and Avouac* [2000] and *Cattin and Avouac* [2000]. The 2015 Gorkha main shock and largest aftershock shown by green stars.

2. The Damak Site

The site is ~10 km north of the city of Damak (Figure 1). Between Mawa and Ratuwa Kholas (Figure 2a) the HFT strikes southeast along a steep ~50 m high escarpment. Repeated thrusting on the HFT is manifest by the presence of at least four relatively smooth and flat fluvial terraces of progressively greater elevation. Each terrace is composed of rounded river gravel capping a Siwalik bedrock strath.

We excavated a trench across the HFT where it strikes ~140° and bounds the youngest terrace adjacent to Ratuwa Khola (Figures 2a, 2b, and S1 in the supporting information). The location of the trench is depicted as the red line on a higher-resolution topographic base map in Figure 2b. Displacement on the HFT here has produced a scarp and led to uplift and abandonment of the youngest T1 surface. The trench was cut on an undisturbed remnant of the scarp. The dissection of the T1 hanging wall surface that is observed immediately behind (northeast) the scarp and locally trends southeast and subparallel to strike probably reflects the presence of folding associated with the creation of the scarp, which is observed in the trench exposure.

3. Structural and Stratigraphic Relationships in the Trench Exposure

3.1. Description

The trench exposed a sequence of fluvial sediments interrupted by thrust motion on a zone dipping ~22° to the northeast (red in Figure 3a). Siwalik bedrock (unit 1) is observed at the base of the exposure on the

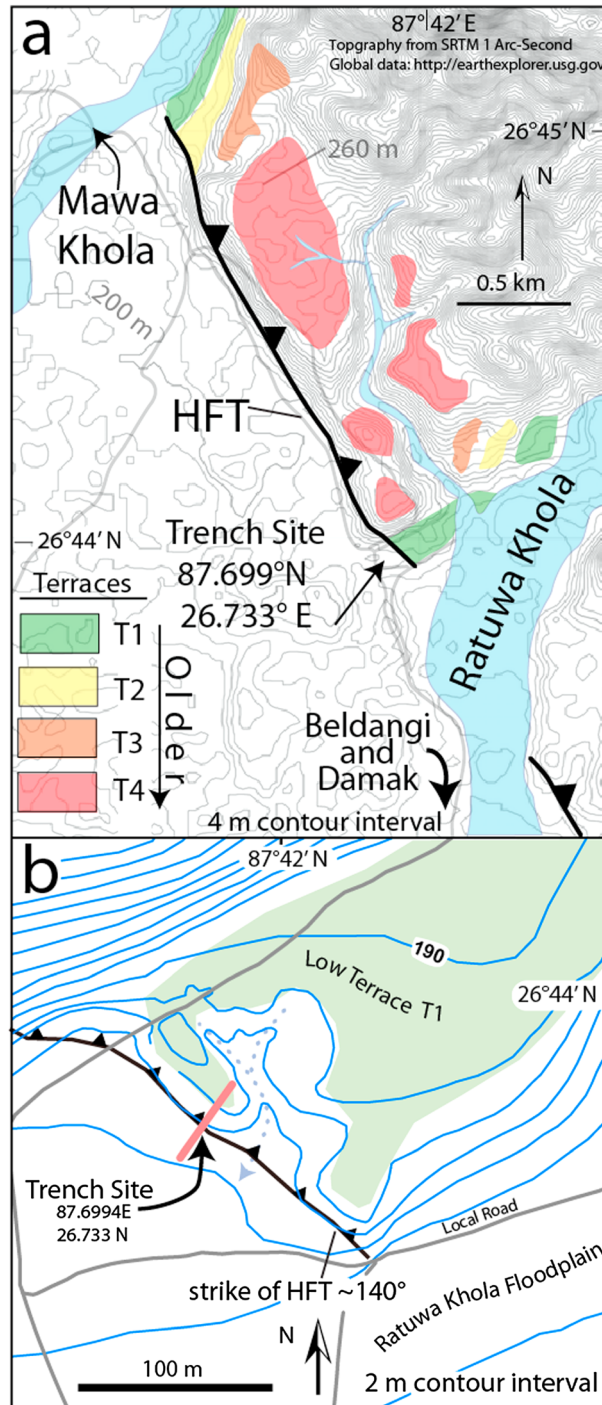


Figure 2. (a) Location of trench. Terrace surfaces identified with field reconnaissance and 1964 vintage aerial photographs. (b) Enlargement of trench site on 2 m contour map constructed with GPS receiver of vertical accuracy of <0.5 m.

hanging wall. The bedrock is overlain by fluvial rounded cobble gravel (unit 2) which, in turn, is capped by an alternating sequence of light brown and tan fine sand and silty sand beds (units 3 to 6). The fluvial layers form an asymmetric fold where the northeastern limb dips gently to the northeast away from the fault and the southwestern limb rolls over more steeply to its intersection with the shear zone. The same sequence of sediments is observed to be flat lying and largely undisturbed on the foot-wall of the scarp. The tan colored unit 7 is located beneath, to the southwest, and above the thrust tip. Darker silt-rich horizons within unit 7 define folded and faulted boundaries of sediment that is similar in composition and color to unit 6. The youngest unit in the exposure is unit 8, a massive dark organic rich silt and very fine sand. Unit descriptions of greater detail are provided in Table S1 in the supporting information. The contact between units 7 and 8 is generally abrupt and defined by a distinct change in color between the two units and the upward termination of the darker silt-rich horizons present in unit 7.

3.2. Interpretation

Units 3–6 are overbank flood deposits accumulated on fluvial gravel of unit 2 (Figure 3a). Horizontal shortening accompanying thrusting resulted in faulting, folding, and duplication of unit 6 and underlying units to produce a “plow zone” (unit 7) at the thrust tip and folding in the hanging wall. Organic rich unit 8 accumulated a thickness of ~2 m subsequent to the displacement that produced the scarp. Vertical separation of unit 2 is 5.5 m. The shear zone dips 22° northeast toward the base of the trench. It is possible that the dip increases to the northeast in the subsurface

beneath the scarp. To reflect the uncertainty in calculations that follow, the dip is allowed to be as steep as 45° below the exposure. For a 22° to 45° dip, about 9.6 ± 4.1 m of horizontal shortening and 11.3 ± 3.5 m of dip-slip motion on the fault plane are needed to produce the observed 5.5 m of vertical separation (Figure 3c). Because fault strike at Damak (140°; Figures 2b and 3c) is oblique to the local

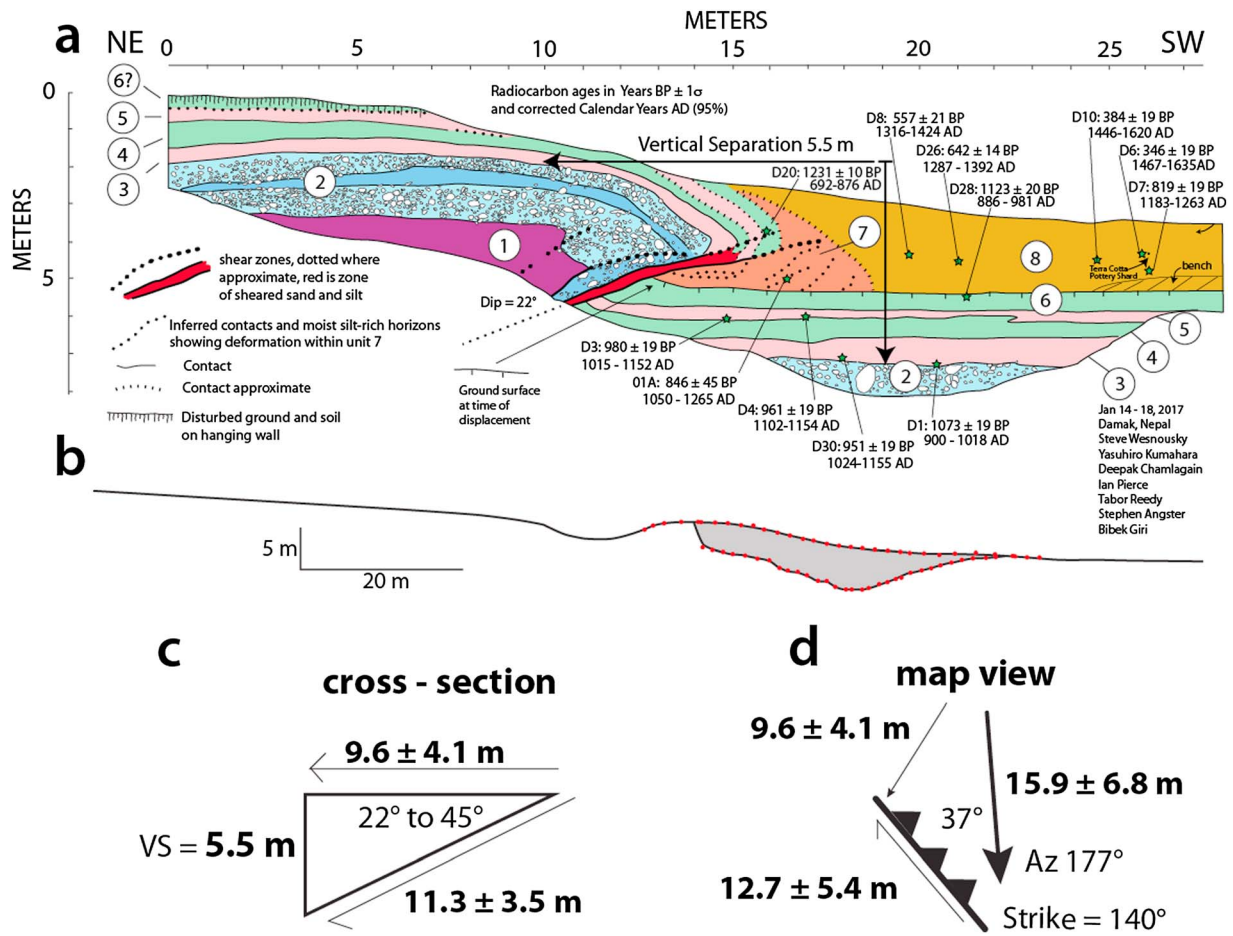


Figure 3. (a) Sketch and (b) profile of trench exposure at Damak. Shading on profile shows location of trench relative to profile. Scarp profile from topographic map constructed with GPS receiver and total station (red dots) with vertical accuracy of ~0.5 m and <3 cm, respectively. (c and d) Geometrical considerations in estimating fault slip. See text.

azimuth of convergence (177°, Figure 1), geometry further predicts that 15.9 ± 6.8 m of horizontal slip parallel to the convergence direction is needed to produce 9.6 ± 4.1 m of fault normal convergence and also leads to the possibility of an additional 12.7 ± 5.4 m of strike slip (Figure 3d). Total slip on the fault plane that produced the observed 5.5 m of vertical separation may in this case be as great as 17.0 ± 6.3 m. We observe no clear evidence of strike-slip motion in the trench exposure although the linearity of the scarp between Mawa

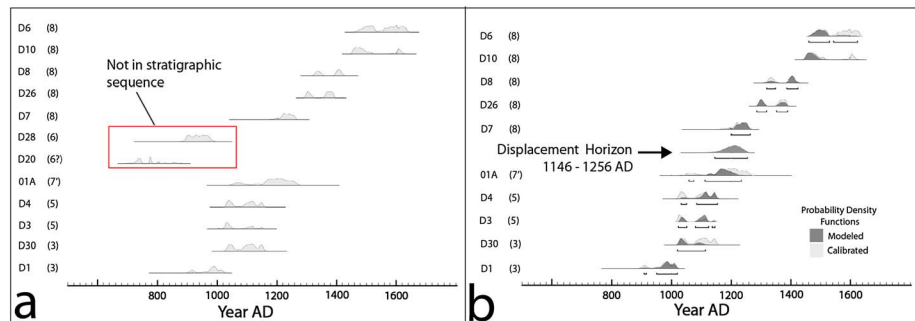


Figure 4. (a) Radiocarbon age probability density distributions of detrital charcoal samples plotted in stratigraphic order. (b) Calibrated and modeled radiocarbon ages excluding samples not in stratigraphic sequence place the displacement horizon at between 1146 and 1256 A.D. Calibration and modeling done with OxCal v4.3.2 (<https://c14.arch.ox.ac.uk/oxcal/OxCal.html>) [Bronk, 2009]) with the IntCal13 atmospheric curve of Reimer et al. [2013].

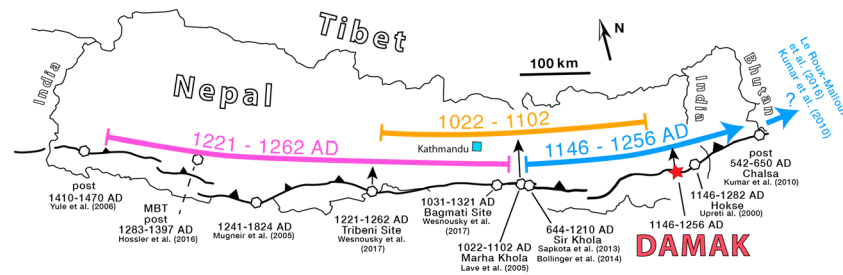


Figure 5. Colored lines delimit the maximum extent of surface rupture for large displacement surface ruptures at Tribeni, Marha Khola, and Damak allowed by paleoearthquake ages reported elsewhere along strike the HFT. Age ranges at Marha Khola and Sir Khola reported by *Wesnousky et al.* [2017] from reanalysis of radiocarbon ages reported in those papers. Age range at Hokse is from reanalysis of radiocarbon ages reported in *Upreti et al.* [2000] and provided in supporting information.

and Ratuwa Kholas allows the possibility. Returning attention to the trench exposure, displacement of unit 4 on and along the shear zone is only about 5 m. The discrepancy reflects an updip transition, whereby slip is increasingly accommodated by folding rather than displacement directly on the fault. Stratigraphic discontinuities and tilting are not present in unit 8, and there exists minimal erosion on the hanging wall. Unit 8 is most simply interpreted to be the result of deposition and soil development after a single earthquake displacement.

Radiocarbon ages of detrital charcoal collected from units 2–7 (broken by the fault) and unit 8 (deposited subsequent to displacement) are shown in Figure 3a and collated in Table S2 in the supporting information. The radiocarbon ages are plotted in the stratigraphic sequence they were collected in Figure 4a. The plot shows that samples D20 and D28 do not satisfy stratigraphic sequence, whereas the remaining samples do. The two detrital charcoal samples appear to be significantly older than the deposits from which they were collected. Excluding samples D20 and D28 yields an estimate of the displacement horizon (that which separates samples in faulted and unfaulted sediments) at between 1146 and 1256 A.D. (Figure 4b).

4. Discussion and Conclusions

Empirical regressions between coseismic displacement, rupture length, rupture width, and M_w from observations of historical earthquakes [e.g., *Blaser et al.*, 2010; *Henry and Das*, 2001; *Leonard*, 2010, 2014; *Strasser et al.*, 2010; *Wells and Coppersmith*, 1994; *Wesnousky*, 2008] provide a framework to consider the possible magnitude and rupture dimensions of the earthquake that produced the 11.3 ± 3.5 m dip-slip offset at Damak. The best fit regressions of average coseismic displacement versus rupture length recently put forth by *Leonard* [2010, 2014] for interplate dip-slip events indicate that an earthquake producing an average of 11.3 ± 3.5 m offset will on average display a rupture length of 450 to >800 km. Similar regressions between rupture length and M_w imply that an earthquake producing a 450 to >800 km rupture length will on average be M_w 8.6 to >9 [*Blaser et al.*, 2010; *Leonard*, 2014; *Strasser et al.*, 2010]. If one asserts that the 11.3 ± 3.5 offset at Damak is a measure of the maximum rather than average slip and assumes, for example, that average offset was closer to ~ 5.5 m, the same scaling laws lead to best estimates of rupture length > 250 km and $M_w > 8.2$. These estimates do not include the possibility of additional strike slip (Figure 3d), in which case the values would be yet larger.

The width of the locked portion of the MHT decollement is about 120 km [*Stevens and Avouac*, 2015, 2016] (Figure 1). Assuming that rupture during the largest events spans the entire width of the MHT decollement, the aspect ratio (rupture length/rupture width) of an 800 km long rupture would be about 7. The aspect ratio of seven falls at the upper bound of what has been observed historically for plate boundary thrust earthquakes [*Henry and Das*, 2001]. Formal regressions between rupture length and width for interplate dip-slip earthquakes [e.g., *Leonard*, 2014, Table 3] show the most likely rupture length for an earthquake rupturing the 120 km width of the MHT decollement is about 600 km. Averaging the 11.3 ± 3.5 m coseismic offset observed at Damak across a fault plane of this dimension is equivalent to an earthquake of M_w 8.7 to >9 ($M_0 = 3e11 \times 100 \text{ km} \times 600 \text{ km} \times (11.3 \pm 3.5 \text{ m})$). If there is additional strike slip, the estimate would be larger.

The locations and estimated ages of earthquake displacements determined in this and other studies along the HFT of Nepal are synoptically shown in Figure 5. We refrain from speculating on possible rupture scenarios [e.g., *Bollinger et al.*, 2014; *Kumar et al.*, 2010; *Wesnousky et al.*, 2017] and limit attention to placing bounds on the maximum length a rupture may have extended from any particular site. Thus, for example, at Damak, radiocarbon ages place the time of displacement at between 1146 and 1256 A.D. Observations in Figure 5 allow that a rupture of this age would not have extended westward of Marha Khola, where the last displacement reportedly occurred 1022–1102 A.D. In the other direction, observations allow the rupture to have extended through Hokse and Chalsa for a cumulative rupture length of ~330 km and perhaps yet another >300 km through sites near Sarpang, Bhutan [*Le Roux-Mallouf et al.*, 2016], and Chalsa and Nameri in eastern India [*Kumar et al.*, 2010]. The 1022–1102 A.D. event at Marha Khola is interpreted by *Lave et al.* [2005] to have 17 m of coseismic displacement. This particular event could have extended no more than 400 km between Tribeni and Damak, where similarly large displacements occurred in 1221–1262 A.D. and 1146–1256 A.D., respectively. In similar fashion, rupture producing an ~15 m displacement at Tribeni between 1221 and 1262 A.D. may have extended a maximum of about 600 km from *Yule et al.*'s [2006] site in far western Nepal to Marha Khola to the east, where bounds on the timing of events are reportedly post-1410–1470 A.D. and 1022–1102 A.D., respectively. The estimated rupture lengths are mutually exclusive and only intended to show that available paleoearthquake observations do not rule out the possibility of very long ruptures implied by the large ~11 m dip-slip offset at Damak. The observations allow a rupture spanning virtually the entire length of Nepal occurred around ~1255 A.D. if, as it has been suggested [*Bollinger et al.*, 2016; *Sapkota et al.*, 2013], radiocarbon dating at Marha and Sir Khola suffers from systematic errors related to inheritance, though it is problematical to make this assumption for only these two sites and not the others.

Geodesists report strain equivalent to about 18 mm/yr of convergence at an azimuth of ~177° is occurring across the Himalayan arc near the longitude of Damak (Figure 1) [e.g., *Ader et al.*, 2012; *Stevens and Avouac*, 2015]. With the assumptions that (1) the rate of strain accumulation is steady through time, (2) that the entirety of slip deficit is stored as elastic energy, and (3) that neither the historical nor geological record is missing evidence of a similarly large displacement on the MHT which produced surface rupture elsewhere on, for example, the Main Boundary Thrust (MBT) rather than the HFT, it may be calculated that the equivalent of ~14.7 ± 1 m of slip has accumulated since 1146–1256 A.D. and is now stored as elastic energy that may be released in an earthquake. It is difficult at best to assess how often or when this strain will be released and whether or not it will all be released in a single earthquake. If the entirety of geodetically measured strain is accommodated as dip-slip displacement at Damak, the time required to accumulate the same amount of displacement as calculated for the 1146–1256 A.D. event is estimated at 531 ± 225 years by dividing 9.6 ± 4.1 m (the horizontal shortening required to produce the scarp at Damak on a fault dipping 22°–45°, Figure 3c) by the ~18 mm/yr of convergence. This is less than the amount of time since 1146–1256 A.D. If one takes into account the obliquity of convergence and assumes that the slip azimuth at the MHT is the same as the azimuth of contraction observed where strain is accumulating to the north, then 15.9 ± 6.8 m of horizontal convergence is required to produce the vertical separation observed across the scarp at Damak (Figure 3d). In this case, dividing 15.9 ± 6.8 m by the ~18 mm/yr convergence rate = 882 ± 375 years is the time required to accumulate the same amount of displacement as occurred in 1146–1256 A.D. The large range of values (531 ± 225 years to 882 ± 375 years) illustrates the large uncertainties in such calculations, which here at Damak are linked largely to lack of knowledge of the fault dip beneath the exposure and the oblique strike of the HFT to the geodetically defined direction of Tibet-India convergence. Uncertainties withstanding, the observations allow that sufficient strain has accumulated along this portion of the Himalayan arc during the 761–861 years since the 1146–1256 A.D. earthquake to produce another earthquake displacement of similar size to that which produced the scarp at Damak. The result compliments earlier, and similar conclusions put forth on the basis of seismic moment budgets, the historical record, and the recognition from geodesy that the MHT is strongly coupled or “locked” [e.g., *Bilham et al.*, 2001; *Bilham and Ambraseys*, 2005; *Stevens and Avouac*, 2015, 2016].

At Marha Khola, Bagmati, and Tribeni to the west of Damak (Figure 1), the most recent surface rupture displacements have been reported to be characterized by similar size and time since their occurrence as those observed at Damak [*Lave et al.*, 2005; *Wesnousky et al.*, 2017]. Those observations led to the analogous conclusion that the section of MHT encompassing the sites is far along in a strain accumulation cycle

leading to another great earthquake. The regions of strong shaking and epicenter of the instrumentally recorded 1934 Bihar earthquake fall within the lesser Himalaya and between Damak and the three sites to the west: Marha Khola, Bagmati, and Tribeni (Figure 1) [Chen and Molnar, 1977; Dunn et al., 1939; Pandey and Molnar, 1988]. Sir Khola is located near the western limit of the strongest 1934 isoseismals. There, Sapkota et al. [2013] interpret radiocarbon ages and displacements observed in trenches and a natural exposure to be compatible with the occurrence of the 1934 earthquake. They further cite some “similarly uplifted hanging wall terraces and ~5 m high free-faced scarps...” as evidence that the 1934 surface rupture extended eastward from Sir Khola for a distance of at least 150 km (red line in Figure 1). Molnar and Deng [1984] reinterpreted waveform spectral densities reported by Chen and Molnar [1977] to estimate the seismic moment of the 1934 event at between 2 and 10×10^{21} N m with a preferred estimate of 4.1×10^{21} N m, the latter equivalent to M_w 8.4. Accepting Sapkota et al.’s estimate of rupture length at 150–200 km and assuming the width of the 1934 rupture was 100 km, the displacement associated with the earthquake would be between about 7 and 9 m if the M_0 were 4.1×10^{21} N m or between 3 and 22 m if the full range of possible M_0 values is considered (displacement = $M_0/\text{length} \times \text{width} \times 3e11$). Assuming that the penultimate earthquake in this region was either 1146–1256 A.D. as observed at Damak or 1022–1102 A.D. as reported at Marha Khola, it may be inferred that a significant amount and perhaps all of the ~18 mm/yr of slip accumulated since that time was released in 1934, in which case the likelihood of another great earthquake in the vicinity of the 1934 rupture may be viewed as less than along adjacent portions of the HFT. It will be important in refining measures of seismic hazard in the region to determine whether or not the ~5 m scarps reported by Sapkota et al. [2013] are indeed the result of the 1934 earthquake.

Acknowledgments

Constructive comments and suggestions of Jean-Phillipe Avouac and Doug Yule improved the manuscript. We thank Andrew Newman for handling of the manuscript. The Department of Forest and District Forest Office (Jhapa), Government of Nepal kindly granted permission for the study, and we are most appreciative of the cooperation extended by Humse-Dumse Community Forest User Group in allowing us to carry out this study. We thank Greg Hodkins and the Arizona AMS laboratory for the high-resolution radiocarbon ages. Radiocarbon data and additional images of study site are archived and accessible in the supporting information. This research supported by National Science Foundation (NSF) grant EAR-1345036. Center for Neotectonics Studies Contribution 73.

References

- Ader, T., et al. (2012), Convergence rate across the Nepal Himalaya and interseismic coupling on the Main Himalayan Thrust: Implications for seismic hazard, *J. Geophys. Res.*, *117*, B04403, doi:10.1029/2011JB009071.
- Ambraseys, N., and D. Jackson (2003), A note on early earthquakes in northern India and southern Tibet, *Curr. Sci.*, *84*, 570–582.
- Avouac, J.-P., L. Meng, S. Wei, T. Wang, and J.-P. Ampuero (2015), Lower edge of locked Main Himalayan Thrust unzipped by the 2015 Gorkha earthquake, *Nat. Geosci.*, *8*, 708–711.
- Bilham, R., and N. Ambraseys (2005), Apparent Himalayan slip deficit from the summation of seismic moments for Himalayan earthquakes, 1500–2000, *Curr. Sci.*, *88*, 1658–1663.
- Bilham, R., K. M. Larson, J. Freymueller, and P. I. members, 1997. GPS measurements of present day convergence across the Nepal Himalaya, *Nature*, *386*, 61–64.
- Bilham, R., V. K. Gaur, and P. Molnar (2001), Earthquakes—Himalayan seismic hazard, *Science*, *293*, 1442–1444.
- Blaser, L., F. Krueger, M. Ohrnberger, and F. Scherbaum (2010), Scaling relations of earthquake source parameter estimates with special focus on Subduction environment, *Bull. Seismol. Soc. Am.*, *100*, 2914–2926.
- Bollinger, L., S. N. Sapkota, P. Tapponnier, Y. Klinger, M. Rizza, J. Van der Woerd, D. R. Tiwari, R. Pandey, A. Bitri, and S. B. de Berc (2014), Estimating the return times of great Himalayan earthquakes in eastern Nepal: Evidence from the Patu and Bardibas strands of the Main Frontal Thrust, *J. Geophys. Res. Solid Earth*, *119*, 7123–7163, doi:10.1002/2014JB010970.
- Bollinger, L., P. Tapponnier, S. N. Sapkota, and Y. Klinger (2016), Slip deficit in central Nepal: Omen for a repeat of the 1344 AD earthquake?, *Earth Planets Space*, *68*, 12.
- Bronk, R. (2009), Bayesian analysis of radiocarbon dates, *Radiocarbon*, *51*, 337–360.
- Cattin, R., and J. P. Avouac (2000), Modeling mountain building and the seismic cycle in the Himalaya of Nepal, *J. Geophys. Res.*, *105*, 13389–13407, doi:10.1029/2000JB900032.
- Chen, W.-P., and P. Molnar (1977), Seismic moments of major earthquakes and the average rate of slip in central Asia, *J. Geophys. Res.*, *82*, 2945–2969.
- Dunn, J. A., J. B. Auden, and A. M. N. Ghosh (1939), The Bihar-Nepal earthquake of 1934, *Mem. Geol. Surv. India*, pp. 27–38 and 210–391.
- Hayes, G. P., et al. (2015), Rapid characterization of the 2015 M_w 7.8 Gorkha, Nepal, earthquake sequence and its seismotectonic context, *Seismol. Res. Lett.*, *86*, 1557–1567.
- Henry, C., and S. Das (2001), Aftershock zones of large shallow earthquakes: Fault dimensions, aftershock area expansion and scaling relations, *Geophys. J. Int.*, *147*, 272–293.
- Kumar, S., S. G. Wesnousky, T. K. Rockwell, R. W. Briggs, V. C. Thakur, and R. Jayagondaperumal (2006), Paleoseismic evidence of great surface rupture earthquakes along the Indian Himalaya, *J. Geophys. Res.*, *111*, B03304, doi:10.1029/2004JB003309.
- Kumar, S., S. G. Wesnousky, R. Jayagondaperumal, T. Nakata, Y. Kumahara, and V. Singh (2010), Paleoseismological evidence of surface faulting along the northeastern Himalayan front, India: Timing, size, and spatial extent of great earthquakes, *J. Geophys. Res.*, *115*, doi:10.1029/2009JB006789.
- Lave, J., and J. P. Avouac (2000), Active folding of fluvial terraces across the Siwaliks Hills, Himalayas of central Nepal, *J. Geophys. Res.*, *105*, 5735–5770, doi:10.1029/1999JB900292.
- Lave, J., D. Yule, S. N. Sapkota, K. Basant, C. Madden, M. Attal, and R. Pandey (2005), Evidence for a Great Medieval Earthquake (~1100 A.D.) in the central Himalayas, Nepal, *Science*, *307*, 1302–1305.
- Le Roux-Mallouf, R., M. Ferry, J. F. Ritz, T. Berthet, R. Cattin, and D. Drukpa (2016), First paleoseismic evidence for great surface-rupturing earthquakes in the Bhutan Himalayas, *J. Geophys. Res. Solid Earth*, *121*, 7271–7283, doi:10.1002/2015JB012733.
- Leonard, M. (2010), Earthquake fault scaling: Self-consistent relating of rupture length, width, average displacement, and moment release, *Bull. Seismol. Soc. Am.*, *100*, 1971–1988.
- Leonard, M. (2014), Self-consistent earthquake fault-scaling relations: Update and extension to stable continental strike-slip faults, *Bull. Seismol. Soc. Am.*, *104*, 2953–2965.

- Molnar, P., and Q. D. Deng (1984), Faulting associated with large earthquakes and the average rate of deformation in central and eastern Asia, *J. Geophys. Res.*, *89*, 6203–6227.
- Mugnier, J. L., P. Huyghe, A. P. Gajurel, and D. Becel (2005), Frontal and piggy-back seismic ruptures in the external thrust belt of western Nepal, *J. Asian Earth Sci.*, *25*, 707–717.
- Nakata, T., B. N. Upreti, Y. Kumahara, H. Yagi, K. Okumura, T. K. Rockwell, and N. S. Virdi (1998), First successful paleoseismic trench study on active faults in the Himalaya, *EOS, trans.*, *79*, F615.
- Pandey, M. R., and P. Molnar (1988), The distribution of intensity of the Bihar-Nepal earthquake of 15 January 1934 and bounds on the extent of the rupture zone, *J. Geol. Soc. of Nepal*, *5*, 22–44.
- Pant, M. R. (2002), *A Step Towards a Historical Seismicity of Nepal*, ADARSA, pp. 29–60, Pundit Publ., Kathmandu.
- Reimer, P. J., et al. (2013), INTCAL13 and marine13 radiocarbon age calibration curves 0–50,000 years Cal Bp, *Radiocarbon*, *55*, 1869–1887.
- Sapkota, S. N., L. Bollinger, Y. Klinger, P. Tapponnier, Y. Gaudemer, and D. Tiwari (2013), Primary surface ruptures of the great Himalayan earthquakes in 1934 and 1255, *Nat. Geosci.*, *6*, 71–76.
- Seeber, L., and J. Armbruster (1981), Great detachment earthquakes along the Himalayan arc and long-term forecasting, in *Earthquake Prediction: An International Review*, edited by D. W. Simpson and P. G. Richards, pp. 215–242, AGU, Washington, D. C.
- Stevens, V. L., and J. P. Avouac (2015), Interseismic coupling on the main Himalayan thrust, *Geophys. Res. Lett.*, *42*, 5828–5837, doi:10.1002/2015GL064845.
- Stevens, V. L., and J. P. Avouac (2016), Millenary $M_w > 9.0$ earthquakes required by geodetic strain in the Himalaya, *Geophys. Res. Lett.*, *43*, 1118–1123, doi:10.1002/2015GL067336.
- Strasser, F. O., M. C. Arango, and J. J. Bommer (2010), Scaling of the source dimensions of Interface and Intraslab Subduction-zone earthquakes with moment magnitude, *Seismol. Res. Lett.*, *81*, 941–950.
- Upreti, B. N., T. Nakata, Y. Kumahara, H. Yagi, K. Okumura, T. K. Rockwell, and N. S. Virdi (2000), The latest active faulting in Southeast Nepal, in *Proceedings of the Hokudan International Symposium and School in Active Faulting*, pp. 533–536, Awaji Island, Hyogo Japan.
- Wells, D. L., and K. J. Coppersmith (1994), New empirical relationships among magnitude, rupture length, rupture width, rupture area, and surface displacement, *Bull. Seismol. Soc. Am.*, *84*, 974–1002.
- Wesnousky, S. G. (2008), Displacement and geometrical characteristics of earthquake surface ruptures: Issues and implications for seismic-hazard analysis and the process of earthquake rupture, *Bull. Seismol. Soc. Am.*, *98*, 1609–1632.
- Wesnousky, S. G., S. Kumar, R. Mohindra, and V. C. Thakur (1999), Uplift and convergence along the Himalayan Frontal Thrust of India, *Tectonics*, *18*, 967–976.
- Wesnousky, S. G., Y. Kumahara, D. Chamlagain, I. K. Pierce, A. Karki, and D. Gautam (2017), Geological observations on large earthquakes along the Himalayan frontal fault near Kathmandu, Nepal, *Earth Planet. Sci. Lett.*, *457*, 366–375.
- Yule, D., S. Dawson, J. Lave, S. N. Sapota, and D. R. Tiwari (2006), Possible Evidence for Surface Rupture of the Main Frontal Thrust During the Great 1505 Himalayan Earthquake, Far-Western Nepal, *EOS Trans. AGU, Fall Meet.*